

4-3 Broadband Millimeter Wave Imaging System

MIZUNO Maya

We developed a system for imaging the dielectric properties of materials in the millimeter range from 30 GHz to 70 GHz. It can observe the distribution of dielectric properties of materials including composites at various frequencies. Experimental results proved that the system clearly observes metal distribution at 35, 45, 55 and 65 GHz, by transmission imaging as well as by reflection imaging. One of the important features in practice is its ability to distinguish water and ice in other materials. The new imaging system can be used to evaluate distribution of dielectric properties of materials in various fields such as engineering and medicine.

Keywords

Millimeter wave, Imaging, Non-destructive inspection

1 Introduction

In recent years we have begun to see the spread of useful daily applications of electromagnetic waves known as millimeter waves. Millimeter waves are radio waves in the wavelength range from 1 mm to 10 mm, which corresponds to a frequency range from 30 GHz to 300 GHz. Taking advantage of the particular characteristics of these waves — their relatively short wavelengths and high frequency among radio waves — millimeter waves have already been applied to in-vehicle radar devices that measure the distance between moving vehicles in order to prevent collisions. These waves have also been applied to high-speed wireless communications at gigabit-level transmission rates[1]. Further, improved generation and detection techniques for millimeter waves have provided additional momentum to research on millimeter-wave imaging applications.

Millimeter waves have a number of characteristics that are similar to those of terahertz waves. For example, millimeter waves easily penetrate non-metal materials, including plas-

tics, walls, clothes, smoke, and fog. The spatial resolution of millimeter waves is, naturally, several millimeters, situating these waves spectrally between microwaves and terahertz waves. Accordingly, millimeter waves can be used in imaging of a diverse array of objects. Studies of various related techniques are underway, such as a passive imaging technique to visualize the image of an individual obscured by flames[2] and a high-sensitivity active imaging technique to reveal guns and knives hidden under clothes[3]. A passive imaging technique creates images of the electromagnetic waves emitted by the objects themselves, by combining millimeter wave antennas, amplifiers, and Schottky diode detectors. An active imaging technique, on the other hand, irradiates millimeter waves to objects and creates images by detecting the transmitted or reflected waves. Trial operations have begun in security applications, including monitoring systems in train stations and airports. Moreover, millimeter waves are sensitive to liquid water. They can identify the water content and frozen condition of liquid at high sensitivity. As a result, expectations are

high for the use of millimeter waves in applications such as monitoring of water content in agricultural crops, moisture content testing of fabrics, and in the observation of freezing and melting cycles of biological samples and frozen food [4].

With respect to the diverse types of imaging described above, a frequency range is selected according to the dielectric properties unique to the target substances or according to the resolution required for the purpose of each application. However, when the sample to be imaged shows individual variability in characteristics (as in the case of living tissues), the frequencies suitable for distinguishing different substances may differ from sample to sample. Cases also arise in which the determination of frequency dependence is sought, as in the case of printed circuit boards. For these applications, a frequency-tunable broadband imaging system is required. Given these characteristics and requirements, our research group attempted to build a broadband millimeter wave imaging system that covers the frequency range from 30 GHz to 70 GHz. This article describes the characteristics of the developed prototype millimeter wave transmission and reflection imaging system and reports on the results of IC card imaging and water/ice discrimination as examples of imaging applications offered by this system.

2 Millimeter wave imaging system

2.1 Configuration of millimeter wave imaging system

Figure 1 shows a schematic diagram of the millimeter wave imaging system. This imaging system uses a network analyzer (Agilent E8363B, 10 MHz – 70 GHz) as the generator and detector. To reduce the size of the system and to improve resolution, horn antennas are not employed to emit the millimeter waves into free space. Instead, a 2.4-mm male coaxial cable connector (Agilent 85133E) is attached to the network analyzer, in addition to a semispherical silicon lens (refractive index of 3.4; diameter of 30 mm) with a focal

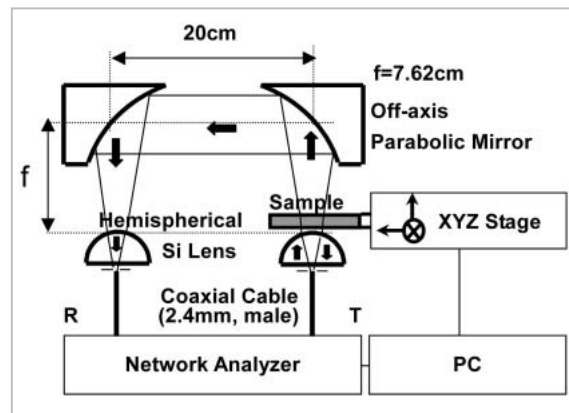


Fig. 1 Schematic diagram of millimeter wave imaging system

length of 6.3 mm, to limit the spread of the millimeter waves irradiated to the sample. The distance between the connector and the lens is 6.3 mm. The reflected waves from the sample are input to the network analyzer through the same port used for the outgoing waves. The waves transmitted through the sample are collected by a parabolic mirror and another silicon semispherical lens and input to the network analyzer through a separate incoming port. Here, the 2.4-mm male coaxial cable connector on the detector side is also placed 6.3 mm from the silicon semispherical lens. In this study the sample is scanned two-dimensionally using an XZ stage; the reflectance and transmittance is then processed by a PC to produce the final image.

2.2 Output characteristics of millimeter wave imaging system

We tested the signal intensity and the beam shape of the developed imaging system. First, we measured the signal intensity values at a transmittance of 100 % and reflectance of 0 % without mounting a sample, and at a transmittance of 0 % and reflectance of 100 % after mounting an aluminum board that blocks electromagnetic waves. Figure 2 shows the measurement results for the transmitted waves. The solid line in the figure indicates the signal intensity at a transmittance of 100 %, and the dotted line indicates the signal intensity at a transmittance of 0 %. The figure shows that placing an aluminum board

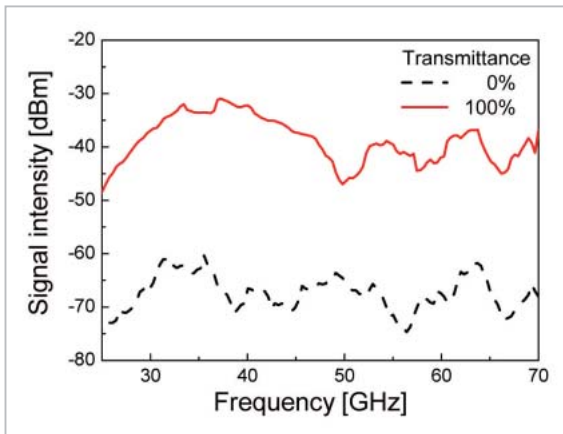


Fig. 2 Signal intensity in transmission imaging

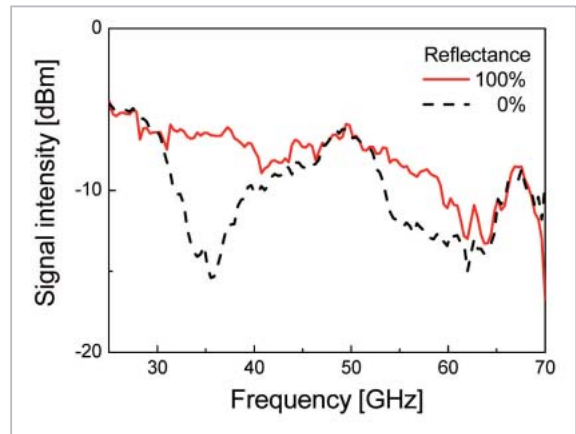


Fig. 3 Signal intensity in reflection imaging

reduces the signal intensity by 20 dB or more in the range from 25 GHz to 70 GHz. It is possible to increase the S/N ratio by narrowing the IF bandwidth of the network analyzer. However, we confirmed that the sweep time must be increased and that the time required to acquire the data increases with a narrower IF bandwidth. The measurement of the reflected waves shows a relatively satisfactory S/N ratio near 35 GHz and 55 GHz, with a maximum value of 10 dB (Fig. 3). Our results have shown that extraction efficiency from the coaxial cable is poor near 50 GHz, which makes it difficult to detect a change in the signal reflected from the sample compared to other frequency ranges.

Next, we checked the beam shape of the millimeter waves irradiated to the sample. We measured the near field pattern of the beam at 35 GHz, 45 GHz, 55 GHz, and 65 GHz at a position approximately 1 mm from the end face of the semispherical silicon lens (Fig. 4). As the beam is emitted from a circular 2.4-mm connector (inner diameter of approximately 6.2 mm), the beam generates a circular interference pattern. We also confirmed that the beam shape is disturbed on the high-frequency side as two or more modes arise when the beam propagates in the connector. The diameters of these zero-order diffraction waves are estimated at 7.8 mm, 12.2 mm, 7.2 mm, and 8 mm, respectively, based on the measurement data. Here, the dark zones of the interference pattern were not clear for the 45-GHz beam,

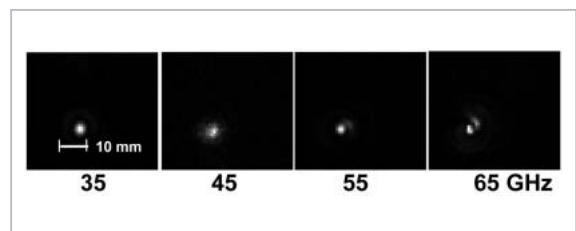


Fig. 4 Near field pattern of beam for each frequency

such that the value may be overestimated for the 45-GHz beam.

2.3 Imaging test

We performed imaging with the developed system. The test sample is comprised of aluminum tape cut into an isosceles right triangle with two sides having a length of 20 mm and attached to a 2.4-mm thick foamed polyethylene sheet (photograph in Fig. 5). The test frequency values used are 35 GHz, 45 GHz, 55 GHz, and 65 GHz. We acquired the transmission and reflection images of 40 mm × 30 mm (with 1-mm steps) at each of these frequencies. The figure confirms the following features. Although the effects of coupling are large for the transmission waves and it is difficult to image the tip of the triangle, the presence of the aluminum tape can be detected at various frequencies. On the other hand, the effects of coupling are small for the reflection waves, and the fluctuation in the intensity is also small. Thus, it is possible to detect slight changes of 2 dB or less, and imaging is possible at frequencies with a low

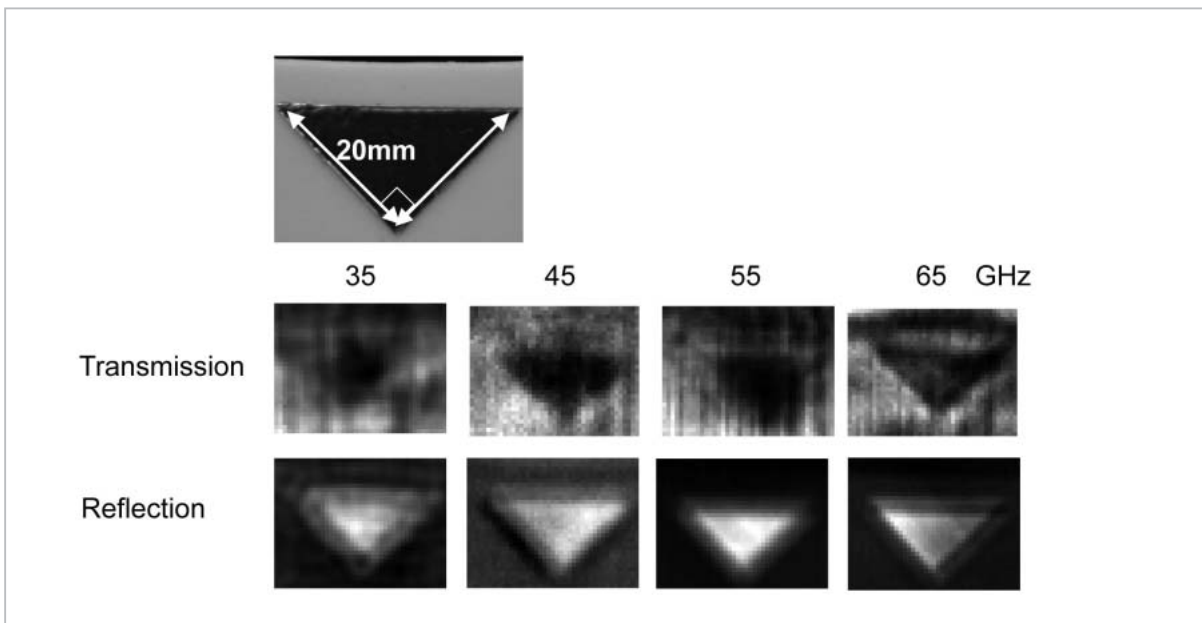


Fig.5 Transmission and reflection images of aluminum tape sample

S/N. In terms of resolution, our general results indicate that higher frequencies produce images with higher resolution with less diffraction when imaging a metal sample. Based on these results, we performed reflection imaging of the NICT IC card at a frequency of 70 GHz, which is the highest frequency possible in this system. Figure 6 shows the results, which confirm that millimeter waves can image the loop antenna and IC chip in the card. These results have demonstrated that this imaging system can produce images over a wide range of different frequencies and allows for evaluation of coupling loop interference or the transmittance and reflectance.

3 Imaging of hidden IC card

We acquired the image of an IC card hidden in foamed polystyrene and checked the effects of the scattering caused by the foamed polystyrene. The sample used is a Suica card from JR East Japan, as its internal antenna structure was already known through terahertz wave imaging[5] and other measurements. The card was placed between foamed polystyrene boards and imaged (Fig. 7). Each of the foamed polystyrene boards was approximately 5 mm thick. Figures 8 and 9 show the

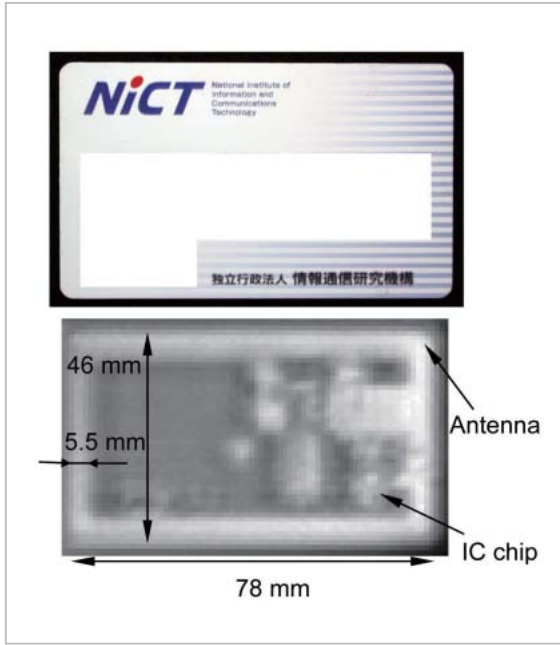


Fig.6 Example of reflection image of IC card (70 GHz)

imaging results at 35 GHz and 60 GHz, respectively. The resultant image is 55 mm × 80 mm. Approximately 60 minutes were required to take an image with 1-mm steps. These figures show that the millimeter waves transmit through opaque materials such as foamed polystyrene and can detect the presence of an antenna hidden inside, both through transmission and reflection imaging. In particular, we



Fig.7 Photograph of imaging sample

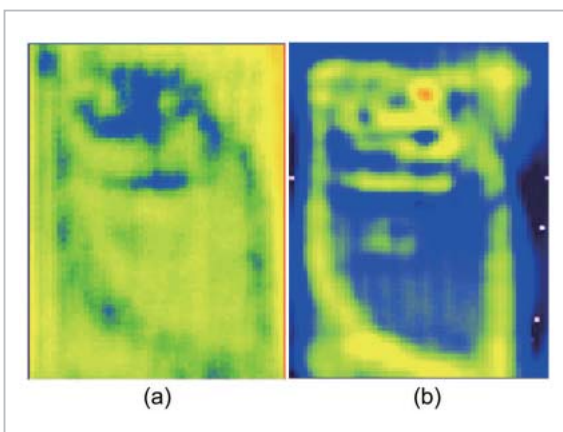


Fig.8 Results of (a) transmission imaging and (b) reflection imaging of Suica card at 35 GHz

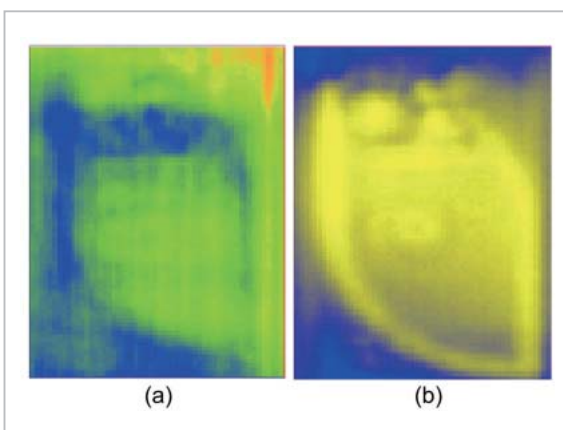


Fig.9 Results of (a) transmission imaging and (b) reflection imaging of Suica card at 60 GHz

confirmed that an image taken via reflection imaging at a frequency of 35 GHz results in the clearest image. While some samples (e.g., metal in a card) can be placed perpendicular to the beam, others cannot be, making reflection imaging sometimes difficult to perform. An image taken at 60 GHz generally shows an

image of the loop antenna and other objects that is less clear than an image taken at 35 GHz, and that the 60-GHz image was distorted in the upper portion. This is because numerous scratches of several millimeters each are present on the foamed polystyrene in the upper portion of the sample, resulting in scattering. After acquiring images at different frequencies, the results have demonstrated that a 35-GHz millimeter wave is less easily influenced by scattering and other effects than a 60-GHz millimeter wave and can more easily measure the characteristics of a sample in uneven foamed polystyrene.

4 Imaging of freezing aqueous solution

Based on the results of the previous section, we performed 35-GHz transmission imaging of water in foamed polystyrene in the solid state and after transition to the liquid state to confirm that the system can detect the difference in the respective dielectric properties depending on the state of a substance. We drilled a hole approximately 1 mm deep into a 1-cm thick foamed polystyrene board and injected the liquid sample into the hole. At the same time, we performed imaging of water mixed with 10 % DMSO (dimethyl sulfoxide; melting point of the mixture is approximately $-4.8\text{ }^{\circ}\text{C}$) in an attempt to detect the difference in the respective dielectric properties of liquid water and the DMSO solution.

Figure 10 (1) shows the results of imaging in the frozen state for a sample placed in a freezer ($-20\text{ }^{\circ}\text{C}$). Here, the transmittance changes slightly as the temperature increases. However, this change is significantly smaller than the change in transmittance (20 dB or greater) arising from the phase transition, such that in this experiment we ignored the effect of temperature on transmittance in the frozen state. Figure 10 (2) shows the results of imaging after allowing this sample to stand at room temperature ($25\text{ }^{\circ}\text{C}$) for 2 hours or more. In both figures, the aqueous solution is shown in the space enclosed with dotted lines. In these

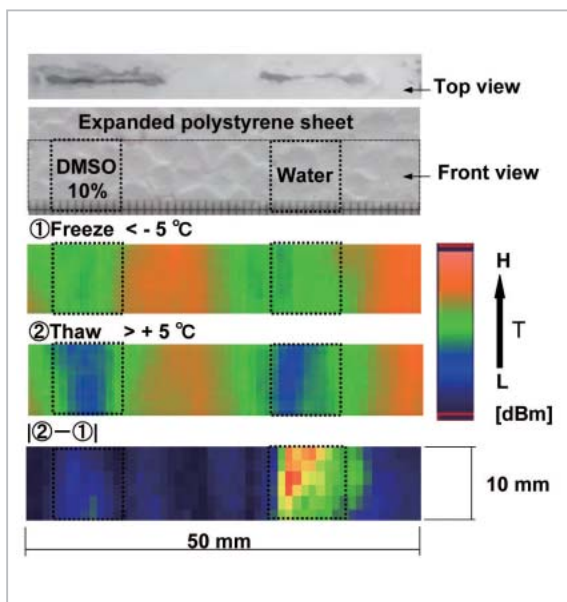


Fig. 10 Results of imaging of water and DMSO solution

figures, we can observe that transmittance decreases when the solution melts. The image obtained by calculating the difference (absolute value) in the transmittance between the liquid and solid phases (Fig. 10, bottom) shows that the difference between these phases in water is larger than that of the DMSO solution. Although we could not detect the slight difference in transmittance between water and the DMSO solution in the images of the frozen and melted states themselves due to the difference in the size (i.e., sample thickness) and shape of the injection hole, we could distinguish water from the DMSO solution by determining the difference between the liquid and solid phases. This result is obtained by making use of the property by which the difference in transmittance between the liquid and solid phases decreases with the addition of DMSO.

These experiments confirm that it is possible to detect a difference in the state of various liquids using 35-GHz transmission imaging. Further, although differences in the shape of the sample and the sample case lead to variation in transmittance, taking the difference in transmittance between different states of the solution can provide a contactless method of distinguishing different samples. These results

indicate the possibility of imaging differences in the dielectric property of various substances using this millimeter wave imaging system.

5 Conclusions

In this study, we built a prototype broadband millimeter wave imaging system and verified its basic characteristics, including broadband performance and signal intensity. We imaged an antenna in a Suica card from JR East Japan placed between two foamed polystyrene boards; the results demonstrated that we can detect metal inside substances opaque to visible light by both transmission and reflection imaging, and that millimeter wave imaging can enable us to observe how the effects of scattering and coupling loop interference differ depending on the imaging frequency.

As an application, we also investigated the possibility of detecting differing dielectric properties between water and ice and between water and a DMSO cryoprotectant solution using 35-GHz transmission imaging. In the case of water and ice, these phases can be distinguished easily due to the large difference in transmittance between the two. In the case of liquid water and DMSO, the difference in transmittance is small, thus it is difficult to distinguish the two solely by comparing transmittance. However, we found that visualizing the difference in transmittance in the liquid and solid phases enables detection even of this slight difference based on the generated images.

These results demonstrate that this system allows for the imaging of samples in opaque materials at various frequencies and that it can provide for comprehensive evaluation, including coupling loop interference, scattering, and dielectric properties of substances. In the future, we intend to improve the broadband performance and imaging accuracy of the system and develop non-destructive inspection systems to detect failures in industrial materials.

References

- 1 H. H. Meinel, "Commercial Applications of Millimeterwaves History, Present Status, and Future Trends", IEEE Transactions on Microwave Theory & Techniques, 43, 1639-1653, 1995.
- 2 K. Mizuno, Y. Wagatsuma, H. Warashina, K. Sawaya, H. Sato, S. Miyanaga, and Y. Yamanaka, "Millimeter-wave imaging technologies and their application", proceedings of IVEC, pp.1-2, 2007.
- 3 D. M. Sheen, D. L. McMakin, and T. E. Hall, "Three-Dimensional Millimeter-Wave Imaging for Concealed Weapon Detection", IEEE Transactions on Microwave Theory and Techniques, 49, 1581-1592, 2001.
- 4 M. Mizuno, C. Otani, K. Kawase, Y. Kurihara, K. Shindo, Y. Ogawa, and H. Matsuki, "Monitoring the frozen state of freezing media by using millimeter waves", Journal of Electromagnetic Waves and Applications, 20, pp.341-349, 2006.
- 5 K. Kawase, "THz-imaging for drug detection and LSI inspection", Optics & Photonics News, 15, 34-39, 2004.

MIZUNO Maya, Ph.D.

*Expert Researcher, Electromagnetic
Compatibility Group, Applied
Electromagnetic Research Center
Applied Electromagnetics*